

Beat M. Riederer, Nathalie Hoffer, Iza Hugonnet,
Raphaël Ayer, Anne Huguenin, Hugues Cadas,
and Silke Grabherr

The use of angiography in the demonstration of vascularization on fresh human cadavers followed by anatomic preparations to visualize structures provides an additional tool for comparing radiographic images with corresponding tissue slices and dissection in undergraduate anatomy teaching. Several regions were investigated in parts as Master's theses to prepare teaching modules to supplement self-directed learning of several regions, i.e., the brain, the heart, the pelvic floor, and knee vascularization [1–4]. A comparison of radiographic images with corresponding tissue slices and three-dimensional (3D) reconstructions of CT scans, as well as the dissection of corresponding anatomic areas, allows a transposition and interpretation of radiographic images by comparison of virtual images with the real anatomic structures.

32.1 Anatomy Education

Anatomy education has undergone considerable changes in recent years. The days of endless lectures are gone, and although lectures still have a place, several studies indicate that learning and retention increase with interactive activities [5–7]. In addition to the traditional ex cathedra lectures and dissection courses, a variety of possibilities are available, such as problem-based learning, small group learning, and web-based instruction [7] as well as the use of plastinated and well-dissected anatomic specimens [8, 9] and radiographic and imaging techniques [6, 10, 11]. Innovative and

multimodal anatomy courses lead to a better performance of medical students [12]. A retrospective study reported that practicing physicians believe that gross anatomy has the highest clinical relevance [13]; however, the most effective way to teach medical anatomy is still debated [14]. Teaching human anatomy to medical students is challenging for several reasons. The 3D organization and the complexity of innervation and vascularization of anatomic structures make it especially difficult to understand the relationship of anatomy with medical or surgical procedures. Therefore, modern imaging techniques can help in learning the structural organization of the human body.

32.1.1 Angiography

Angiography or arteriography is an imaging technique that allows the visualization of blood vessels and organs. It is used widely in medical procedures to visualize vascularization of the brain after a stroke; in coronary angiograms to identify responsible arteries after a cardiac infarction; to identify aneurysms; and most important, as a rapid intervention after insult [15–17]. Recent developments of performing pumps have extended the application of 3D angiography on cadavers, allowing visualization of the arterial and venous systems and to introduce this technique to undergraduate anatomy teaching as well as forensic medicine. This use enables students to become familiar with anatomic structures as soon as possible by comparing morphologic dissection with body slices and analysis of CT scans. Recent advances in postmortem angiography allow for reconstruction of blood vessels in cadavers, followed by dissection and preparation of tissue slices to transpose radiographic images and 3D reconstructions to matching structures in tissue slices or dissected parts. These modern imaging techniques complete the panel of teaching tools such as ex cathedra courses, problem-based learning, dissections, self-directed learning, demonstrations, and the use of prosected specimens and plastinated preparations. Students express difficulties even in clinical

B.M. Riederer, PhD, PD (✉) • N. Hoffer, MD • I. Hugonnet, MD
R. Ayer, MD • A. Huguenin, MD • H. Cadas, PhD
Platform of Morphology, Faculty of Biology and Medicine,
University of Lausanne, Lausanne, Switzerland
e-mail: beat.riederer@unil.ch; Nathalie.Hoffer@unil.ch;
Iza.Hugonnet@unil.ch; Raphael.Ayer@unil.ch;
Anne.Huguenin@unil.ch; Hugues.Cadas@unil.ch

S. Grabherr, MD, PhD
Departement of Forensic Imaging, University Center of Legal
Medicine Lausanne-Geneva, Lausanne, Switzerland
e-mail: silke.grabherr@chuv.ch

semesters with transposing morphologic anatomy and radiographic images. Therefore, we decided to complement pre-clinical teaching with radiographic images and corresponding anatomic preparations of the same body to allow a transition from two-dimensional (2D) visualizations in scans and slices to 3D reconstructions and anatomic dissections.

32.1.2 Master's Studies on Human Cadavers by CT Imaging, Angiography, Dissection, and Preparation of Anatomic Slices

In Europe, the Bologna system requires that medical students provide a Master's thesis before they can take the medical board examination. At the University of Lausanne, we involved several students in establishing novel teaching techniques, including radiographic imaging, angiography, and tissue preparation to supplement preclinical teaching modules for undergraduates. Projects involved human cadavers and standard imaging techniques, followed by anatomic preparation of selected regions to set up teaching modules for first- and second-year medical students. Several cadavers were used, either in parts (pelvis only) or by whole body radiography by injection through femoral arteries and veins for the upper part (head, plexus, heart, and pelvis angiography) or for the lower limb (knee angiography) [1–4]. An important point in the preparation of this type of teaching in small groups was to show the clinical relevance of the region and not to present a list of anatomic structures to identify.

32.2 Methodology

32.2.1 Human Bodies

Bodies were obtained from the local donation program at the Platform of Morphology. Each person had given informed written consent. Three human cadavers were used for the preparation. In one case, a fixed pelvis was scanned by computed tomography (CT) (Fig. 32.1) and by magnetic resonance imaging (MRI) and then dissected, with one side innervation only and the other side with organs in place. Two fresh female cadavers were first scanned by CT, with injection of the contrast liquid Angiofil (USN Center; Satellite Beach, FL). The scanning procedures are documented photographically in Figs. 32.2, 32.3, 32.4, 32.5, 32.6 and 32.7. Subsequently, the first body was fixed with standard fixation [9] and kept at 8 °C for 1 month before dissection and slicing of the pelvis were initiated [2]. For preparation of slices, the pelvis was frozen at –20 °C and cut with a band saw into two equal halves; the right side was dissected and the other side was used for slicing and matching to CT scans. Unfortunately, both bodies had a hip prosthesis on one side, so the right side with a prosthesis in place was used for dissection and the other side was cut into slices 3-cm thick for a comparison of CT scans and corresponding body slices. For the knee vascularization, femoral arteries and veins of a fresh cadaver were catheterized downward and scanned. Both knees were cut proximally and distally and used for injection of red and blue polyester (a two-component paint that polymerizes within 30 min once the two components are combined), followed by fixation in alcohol and dissection or slicing.

32.2.1.1 Imaging

Acquisition of scans was done with a Multi-Detector Computed Tomography (MDCT) Light Speed Ultra (eight rows; GE Medical Systems, Milwaukee, WI). The following parameters were used: 120 kV; 200 mAs; field of view (FOV), 40; section thickness, 1.25 mm; and reconstruction interval, 0.7 mm, pitch 1.35 for the fixed pelvis. The second body was fresh (postmortem interval, ~1 day), and cannulas were placed in the femoral artery and vein. A recently developed pressure-controlled perfusion device (Virtangio, Fumedica AG, Switzerland) was used to inject a mixture of contrast agent (Angiofil) and paraffin oil (paraffinum liquidum, obtained from a local pharmacy) following the protocol proposed by Grabherr and coworkers [18–20]. The arterial phase of Multi-phase Postmortem CT Angiography (MPMCTA) was carried out using the following scan parameters: FOV, 50 cm; slice thickness, 1.25 mm; and interval of reconstruction, 0.6 mm, 120 kVp, 280 mA. Scan parameters for the venous and dynamic phases were as follows: FOV, 50 cm; slice thickness, 2.5 mm; and interval of reconstruction, 1.2 mm, 120 kVp, 280 mA.

The reformatted images were then transferred to a GE Advantage Workstation (version 4.0), where 2D coronal and sagittal views were obtained at 0.5-mm intervals and

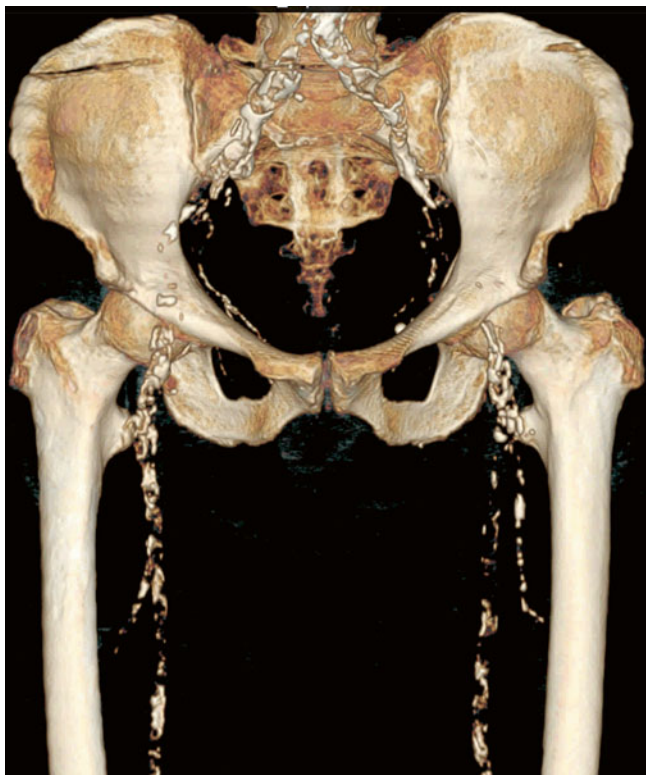


Fig. 32.1 Arteriosclerosis of the iliac and femoral arteries. 3D-volume-rendering (VR) reconstruction of a native MDCT of a female pelvis shows a considerable degree of atherosclerosis in the iliac and femoral arteries

photographed with a wide window width of 3500 UH, centered at +400 UH to enable a precise analysis of the bony structures. Surgical interventions were executed under a dissection microscope and by endoscopic control. CT scans were also made after surgery and after plastination. MRI acquisition was done at the local university hospital with an MRI Siemens TRIO 3 T gradient 40 T/m using a six-channel body array flex coil.

32.2.1.2 Polyester Injection, Slicing, and Dissection

Injection of colored polymers was performed as previously described [21, 22]. The heart was plastinated by the standard method with S-10 silicone, first by dehydration with a graded series of alcohols, followed by acetone and forced polymer impregnation with S-10 silicone (Biodur, Carpenter Technology Corp, Wyomissing, PA) [9, 23]. For the injection of resins into the popliteal artery and veins, a two-component polyurethane topside paint (yachtpaint.com; International AkzoNobel: Rochelle Red S299 and Flag Blue K990) was injected right after the scanning and prior to fixation with alcohol. The right knee was used for slicing and the left knee for the dissection of genicular arteries.



Fig. 32.2 MDCT scanner at the CURML (Centre Universitaire Romand de Médecine Légale). The forensic team discusses the procedure for scanning a female pelvis, which is placed on the MDCT table

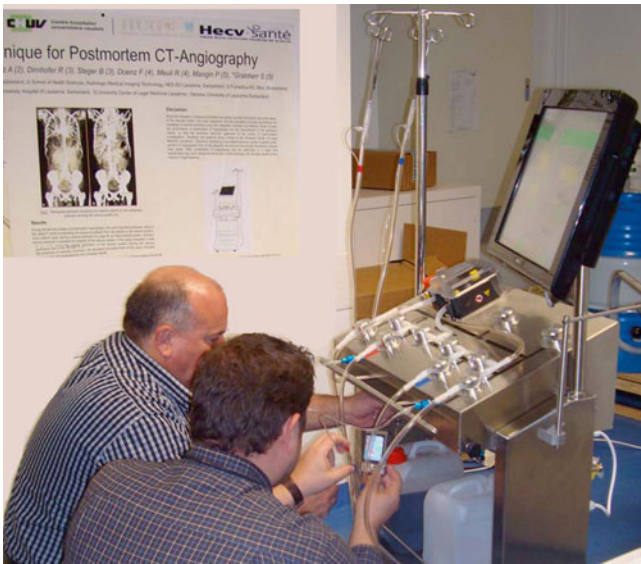


Fig. 32.3 First installation of the pump for arterial and venous circulation, done by the forensic radiographer with the help of the engineer who developed the prototype



Fig. 32.5 Scanning of a female pelvis, which is placed on the MDCT table inside a plastic cover



Fig. 32.4 Preparation of the injection site by placement of catheters into femoral arteries and veins, done by the forensic radiographer

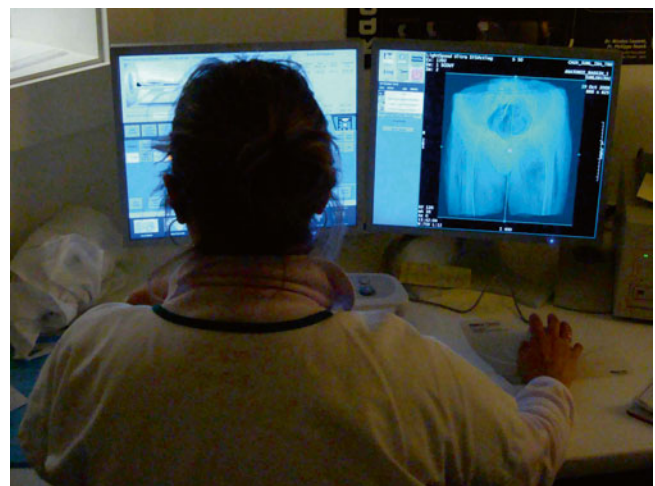


Fig. 32.6 Workstation for the CT scanner, showing the positioning (Scout) of the female pelvis on the *right screen*



Fig. 32.7 Preparation of the pelvis for MRI at the University Hospital in Lausanne

32.3 Results

Three-dimensional CT scans and angiography of several body parts provided magnificent images and 3D reconstructions of vascularization. Together with anatomic slices and dissections, a good comparison between virtual images and the real anatomic structures was possible.

32.3.1 Brain Angiography and the Circle of Willis

The circle of Willis was first described in 1664 [24, 25] and documents that brain vascularization was known for a long time. Angiography provides an ideal means to visualize the complex vascularization of the brain (Fig. 32.8), with the anterior, middle, and posterior cerebral arteries (Figs. 32.9 and 32.10). These arteries are also seen in virtual slices (Fig. 32.11). Of particular interest are the carotid arteries with their ramifications. An artery cast of an isolated brain shows the polygon at the base of the brain (Fig. 32.12) and as a CT scan after angiography (Fig. 32.13). A circle of Willis on display in a jar is shown in Fig. 32.14, and a 3D CT angiogram of the circle of Willis is shown in Fig. 32.15. This comparison of carefully dissected and colored arteries and angiography provides an excellent means of identifying and learning about the vascularization of different brain areas. In view of the clinical application, this technique is especially important for approaching the brain vascularization by angiography; identifying a deficient vascularization, obstructed arteries, and hemorrhages; and dissolving blood clots in obstructed arteries with living angiography and without having to open the skull [26].

32.3.1.1 Brachial and Cervical Plexus

The presentation of the brachial plexus was in preparation during the writing of this chapter [4]. The master thesis was finished in early 2015 and Anne Huguenin received a distinction from the Faculty of Biology and Medicine of the University of Lausanne. There are two plexi, the cervical plexus more superficially in the neck region and the brachial plexus situated around the axillary and brachial arteries. The left side of the neck region shows the carotid artery in a lateral (Fig. 32.16) and frontal view (Fig. 32.17). With the addition of more soft tissue, the sternocleidomastoid becomes visible (Fig. 32.18). Nervous tissue is not seen in this 3D-CT, but the localization of the cervical plexus may be suspected near the artery. Only a dissection of this region shows the complexity of the punctum nervosum with different nerves (Fig. 32.19).

Angiograms of the right shoulder were prepared, showing circumflex scapular arteries (Figs. 32.20 and 32.21). It is important to understand the principle of the formation of the plexus, from roots, trunk, divisions, cords, and nerve ramifica-

tion (Fig. 32.22). Observe the superior and middle trunks near the scalenus muscle and subclavian artery; anterior and hidden posterior divisions; lateral and medial cords and posterior cord, hidden behind the axillary artery; and the musculocutaneous, median nerves, and ulnar nerve (hidden by the median nerve) as well as the axillary and radial nerves. The brachial plexus first surrounds the subclavian artery and continues, surrounding the axillary artery and then the brachial artery (Fig. 32.22).

32.3.1.2 Heart Angiography

Among the most common angiograms performed to visualize arteries are those of the heart to identify coronary arteries. In the living patient, a flexible catheter is used to administer a contrast agent, followed by identification of major coronary arteries by conventional x-rays, MDCT, or MRI to identify unperfused regions or obstructed arteries. In cadavers, the heart has stopped, and the radiopaque liquid must be pumped through the vascular system, a technique that is often used in medico-legal cases [19, 20] with differences in the choice of contrast agents [18]. The heart in situ is shown in Fig. 32.23 in a 3D model of the CT angiogram (*left*). The same heart was isolated, dissected, and plastinated (Fig. 32.23, *right*).

32.3.1.3 Pelvic Angiography

Teaching the female pelvic floor anatomy to medical students is one of the more difficult topics. This difficulty arises on the one hand because of the 3D organization and the complexity of different levels, including the pelvic diaphragm, and on the other hand because of the transition between the abdominal cavity and the pelvic floor. Although it may be too early to introduce medical imaging in the first and second years, a comparative approach with a traditional dissection of human corpses and a virtual approach with the same specimen bear several advantages for identification of essential structures. Having both scans and real slices of the same body available facilitates comparison of virtual images and real anatomic structures. This multimodal approach helps to consolidate anatomic knowledge during early anatomy studies, which is especially important for transposing from a 2D representation of scans and slices into a 3D view. Two projects consisted of setting up a self-directed teaching post using medical imaging and dissected and sliced samples of female pelvises. A pelvis with severe atherosclerosis that was impossible to perfuse was scanned and used for CT reconstruction (*see* Fig. 32.1). A CT and an MRI scan at the level of the trochanter minor are shown in Figs. 32.24 and 32.25. Note the fine resolution of soft tissue and structures such as the external sphincter of the urethra and the vagina

and rectal ampulla. The prior fixation affected the tissue and made it somewhat brighter (hyperintense) on MRI.

Angiography was performed on a second body (the same body as for the head and neck, arms, and heart). The angiogram of the pelvis (Fig. 32.26) shows the catheters placed in the left femoral artery and vein. The left half of the pelvis was cut into slices, and corresponding CT scans were matched and labeled (Figs. 32.27, 32.28, 32.29, 32.30, 32.31, and 32.32). The hip prosthesis on the right side produced some radiation artifact but still allowed identification of anatomic structures in scans and slices. The right half of the pelvis was dissected (Fig. 32.33). A 3D-CT angiogram shows the blood vessels of the same female pelvis (Fig. 32.34). These preparations were introduced in the second year of the medical curriculum in self-directed learning of pelvic floor anatomy. In addition, several critical regions were discussed in relation to stress-induced urinary incontinence, prolapse, hysterectomy, and nerve compression to demonstrate the importance of the pelvic anatomy [8, 27–30]. Note the difference in the vascularization of the anal region (*asterisk* in Fig. 32.34) with the presence of accessory inferior rectal blood vessels on the right side only (No. 8). Accessory blood vessels are often accompanied by perineal nerves and characterized by a passage in the pudendal canal, which can be susceptible to nerve compression, causing pelvic pain [30].

32.3.1.4 Vascularization of the Knee

Bony structures, soft tissue, and the relation of structures are shown in Figs. 32.35, 32.36, and 32.37. MDCT angiograms and slices of a knee were prepared. Prior to slicing of the knee, a two-component polyurethane lacquer (red and blue) was injected into the popliteal artery and vein. Slices and MDCT scans were matched (Fig. 32.38 with matching levels and figures indicated to the right). The most frequent organization is a medial and a lateral superior genicular artery, a single medial genicular artery, and a medial and a lateral inferior genicular artery. In addition, from the femoral artery comes a descending genicular artery, and from the anterior tibial artery, a recurrent artery. Furthermore, there are two muscular arteries for the gastrocnemius muscles [31]. Corresponding levels are shown in Figs. 32.39, 32.40, 32.41, 32.42, 32.43, 32.44, 32.45, 32.46, 32.47, and 32.48. Some of the genicular arteries are seen on CT scans. An angiogram of the left knee (Fig. 32.49) and a 3D-CT angiogram (Fig. 32.50) are shown. Note that the smaller blood vessels were difficult to reconstruct, despite the fact that they were not obstructed and were visible after injection of red two-component paint (Figs. 32.40, 32.42 and 32.44).

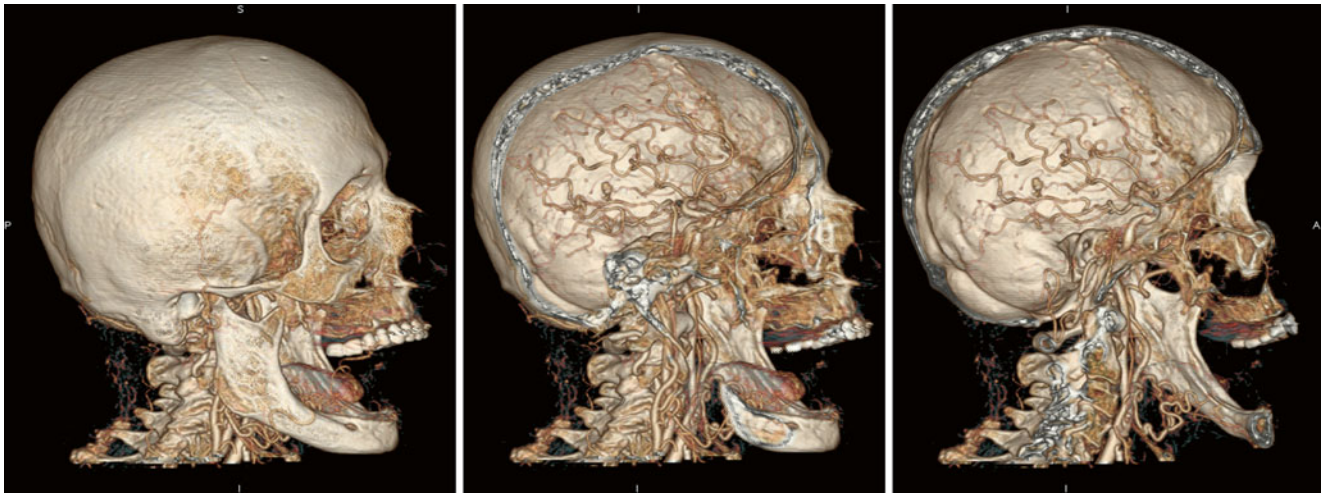


Fig. 32.8 3D-VR reconstruction of head arteries visible from external to internal (*left to right*)

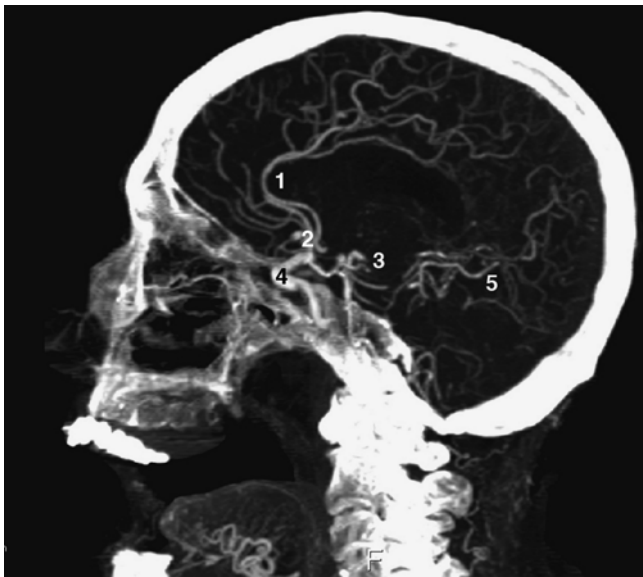


Fig. 32.9 Maximum-intensity projection (MIP) of the arterial phase of brain angiography by lateral view and circle of Willis. (1) Anterior cerebral artery; (2) anterior communicating artery; (3) middle cerebral artery; (4) internal carotid artery; (5) posterior cerebral artery

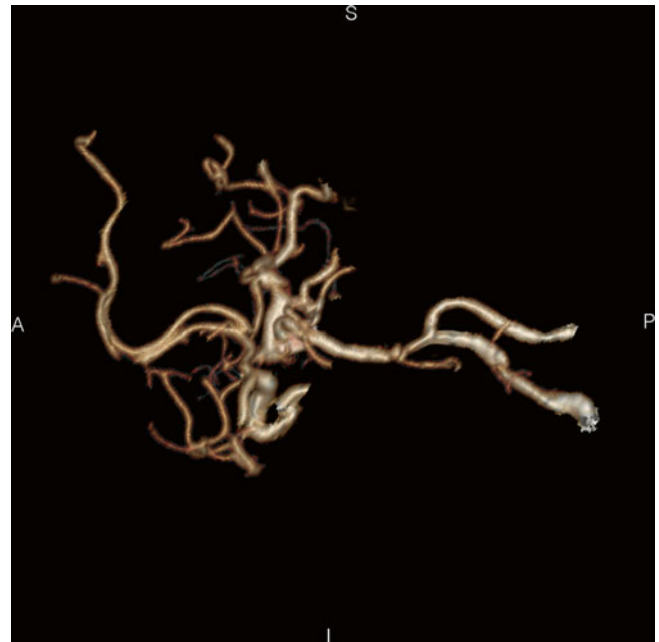


Fig. 32.10 3D-VR reconstruction of circle of Willis, lateral view

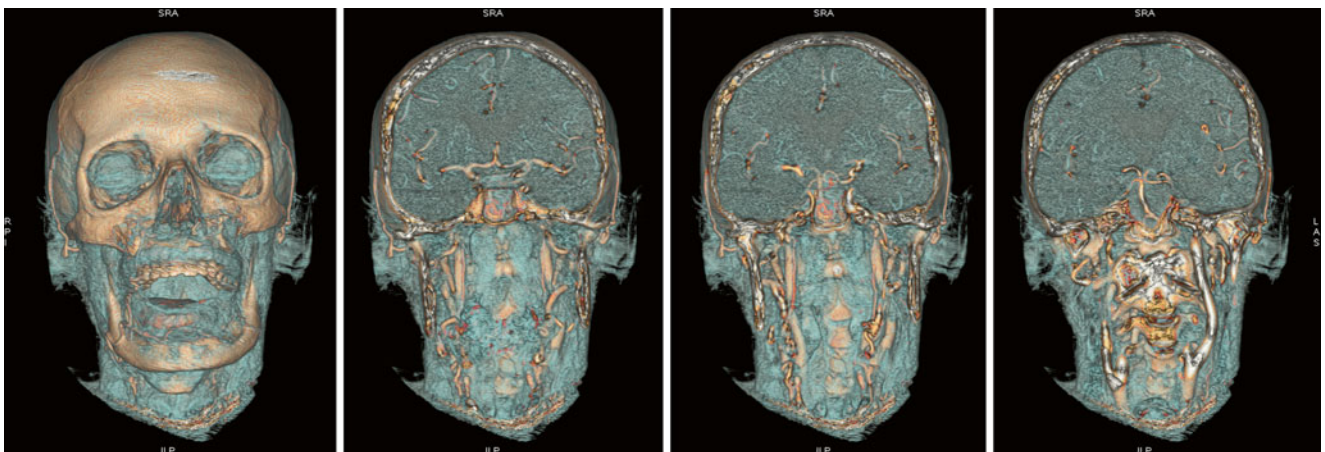


Fig. 32.11 3D-VR reconstructions in a frontal view of the head with soft tissue windowing in frontal sections from anterior to posterior (*from left to right*). Note the different parts of the circle of Willis, the anterior and middle cerebral arteries, and the basilar artery

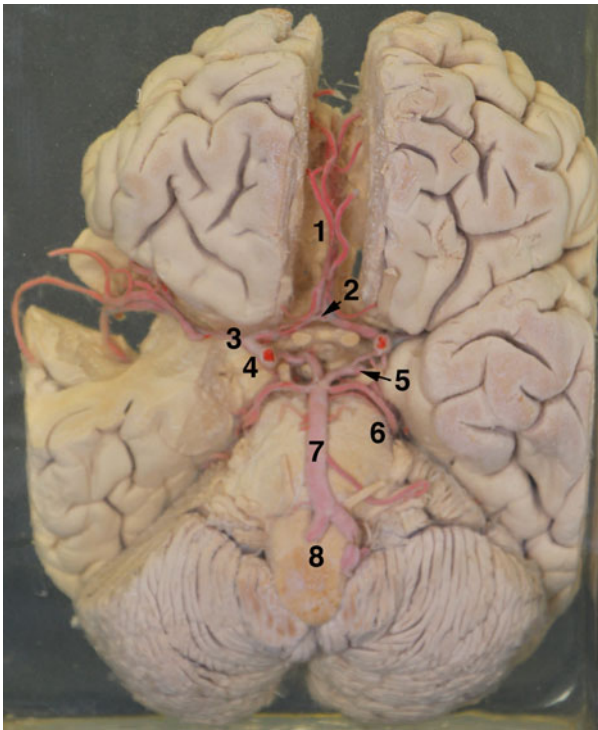


Fig. 32.12 The cerebral arteries viewed from the basal side with the circle of Willis isolated. An artery cast was made with red. (1) Anterior cerebral artery; (2) anterior communicating artery; (3) middle cerebral artery; (4) internal carotid artery; (5) posterior cerebral artery; (6) superior cerebellar artery; (7) basilar artery; (8) vertebral artery

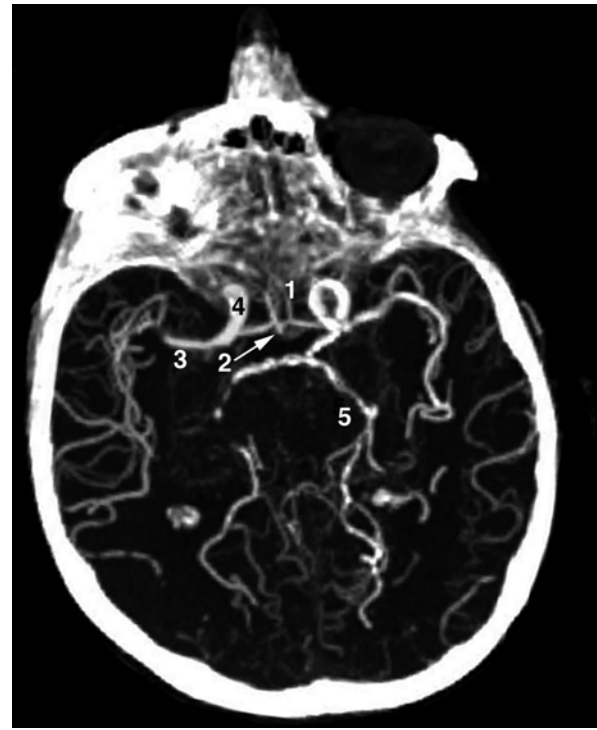


Fig. 32.13 Axial MIP reconstruction of the arterial phase of CT angiography showing the circle of Willis. (1) Anterior cerebral artery; (2) anterior communicating artery; (3) middle cerebral artery; (4) internal carotid artery; (5) posterior cerebral artery

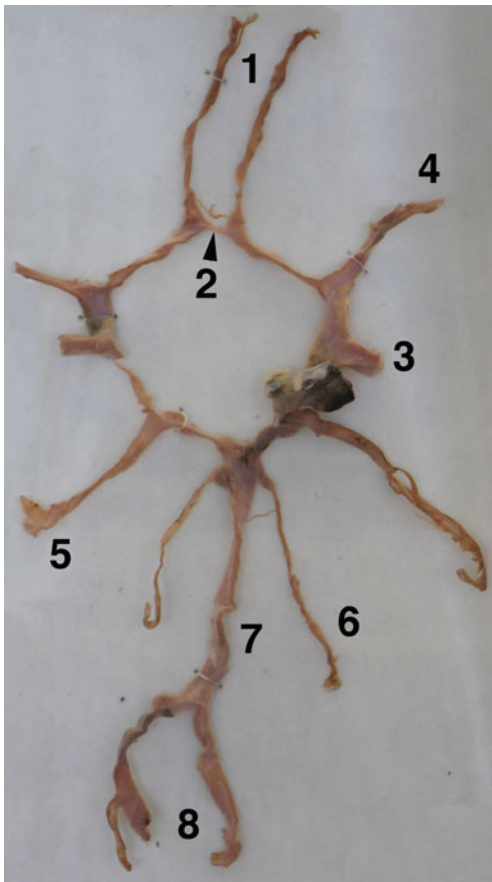


Fig. 32.15 3D-VR reconstruction of the circle of Willis in the arterial phase of MPMCTA

Fig. 32.14 Isolated circle of Willis demonstrating the polygonal form of the anastomoses. (1) Anterior cerebral artery; (2) anterior communicating artery; (3) middle cerebral artery; (4) internal carotid artery; (5) posterior cerebral artery; (6) superior cerebellar artery; (7) basilar artery; (8) vertebral artery



Fig. 32.16 3D-VR reconstruction of the arterial phase of postmortem angiography showing the lateral view of the left side of the head and neck region

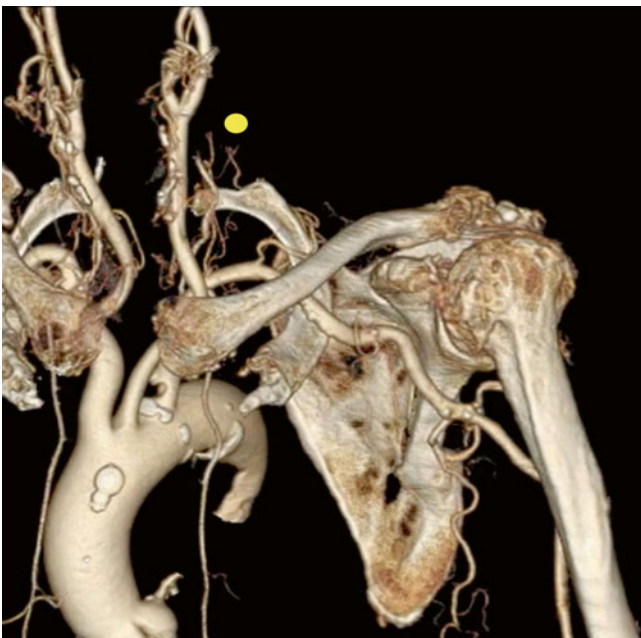


Fig. 32.17 View of the carotid and axillary arteries in a 3D-VR reconstruction of the arterial phase of postmortem angiography. The yellow spot indicates the punctum nervosum



Fig. 32.18 Anterolateral view of a 3D-VR soft tissue reconstruction of the arterial phase of postmortem angiography of the neck with a presentation of the sternocleidomastoid muscles. Note also the facial and temporal arteries and the artery leading from the punctum nervosum (yellow spot) to the trapezius

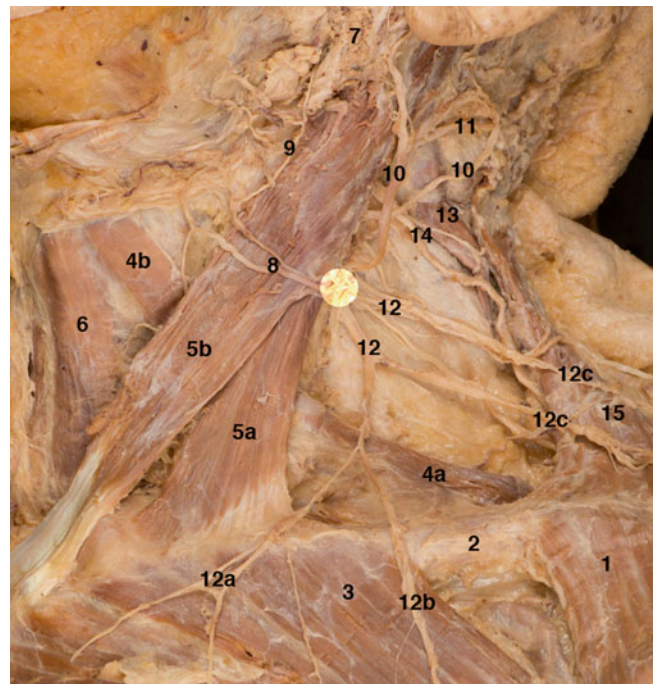


Fig. 32.19 Dissected left cervical plexus with punctum nervosum (yellow spot), anterolateral view. (1) deltoid; (2) clavicle; (3) pectoralis major; (4) omohyoid; (a) pars inferior, (b) pars superior; (5) sternocleidomastoid with (a) clavicular and (b) sternal insertion; (6) sternohyoid; (7) parotid gland; (8) transverse nerve of the neck, with (9) anastomosis with facial nerve; (10) greater auricular nerve; (11) occipitalis minor nerve; (12) supraclavian nerves with (a) medial, (b) intermediate, and (c) lateral branches; (13) splenius capitis; (14) accessory nerve; (15) trapezius



Fig. 32.20 3D-VR reconstruction of the arterial phase of postmortem angiography of the right shoulder with passage of the brachial artery and circumflex and subscapular arteries. Note that the clavicle was fractured

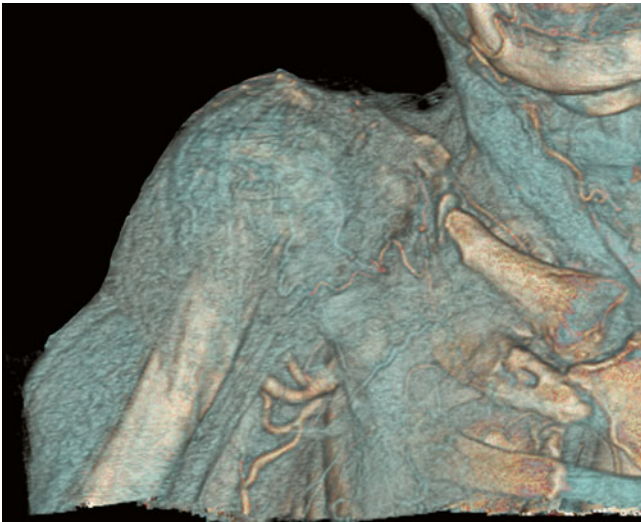


Fig. 32.21 The same view as in Fig. 32.19 but with muscles in place (3D-VR soft tissue reconstruction of the arterial phase of postmortem angiography): deltoid, pectoralis major, and coraco-brachialis

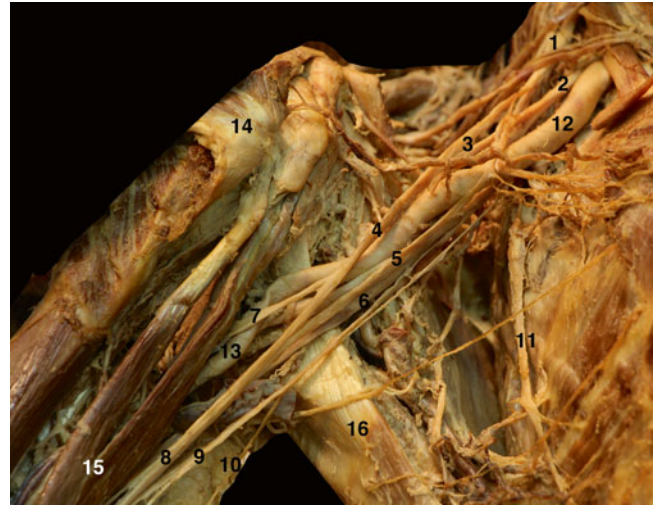


Fig. 32.22 Brachial plexus surrounds axillary and brachial artery. (1) Superior trunk; (2) middle trunk; (3) anterior divisions; (4) lateral cord; (5) medial cord; (6) posterior cord; (7) musculocutaneous nerve; (8) median nerve; (9) medial brachial cutaneous nerve; (10) medial antebrachial cutaneous nerve; (11) long thoracic nerve; (12) subclavian artery; (13) brachial artery; (14) pectoralis major; (15) biceps brachialis; (16) latissimus dorsi

Fig. 32.23 Anterior view of the heart in situ, after angiography and 3D-VR reconstruction of the dynamic phase of MPMCTA (*left*) and after isolation, dissection, and plastination (*right*). (1) superior vena cava; (2) right atrium; (3) right ventricle; (4) pulmonary sinus; (5) pulmonary trunk; (6) pulmonary veins; (7) left ventricle; (8) ascending aorta; (9) left coronary artery; (10) circumflex branch; (11) interventricular artery; (12) right coronary artery; (13) brachiocephalic artery; (14) carotid artery; (15) subclavian artery; (16) ductus arteriosus; (17) descending aorta

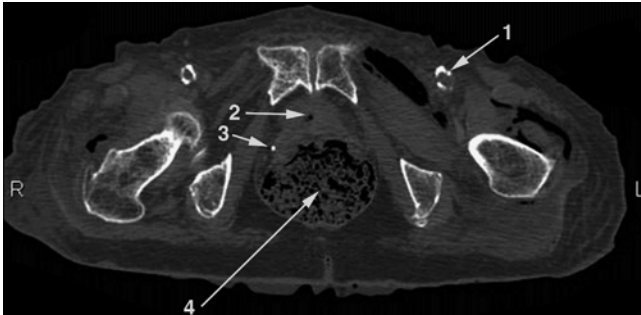
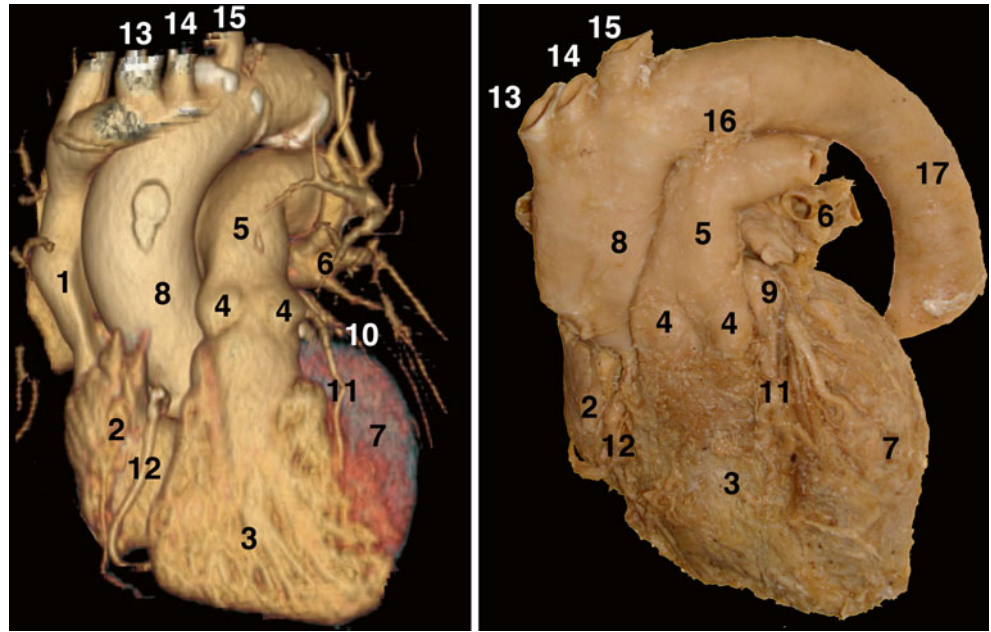


Fig. 32.24 Axial image of native MDCT of the sclerotic pelvis, pubis, trochanter minor, and ischion. (1) Femoral artery; (2) urethra; (3) pudendal artery; (4) rectal ampulla (*R* right, *L* left)

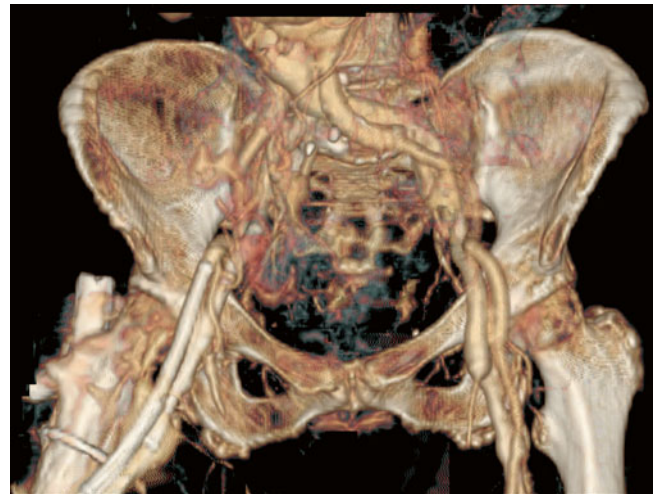


Fig. 32.26 3D-VR reconstruction of the venous phase of the pelvis. Note the catheters inserted into the right femoral artery and vein. The right femur head is replaced by a prosthesis. The *left side* was cut in horizontal slices for a comparison with corresponding CT scans (Figs. 32.27, 32.28, 32.29, 32.30, 32.31, and 32.32), while the *right side* of the pelvis was dissected (see Fig. 32.33). The blood vessels were reconstructed in Fig. 32.34

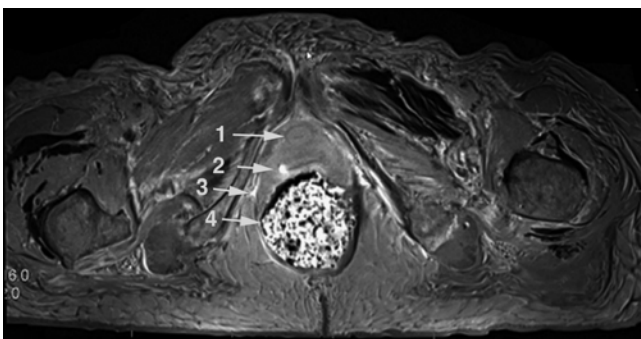


Fig. 32.25 Axial MRI image of the same pelvis at the same level. Because the pelvis was fixed (formalin, alcohol, and glycerol), the contrast of structures was less obvious. However, (1) urethra with external sphincter, (2) vagina with artery, (3) pudendal artery, and (4) rectal ampulla are distinguishable



Fig. 32.27 Axial MDCT reconstruction of the arterial phase of MPMCTA at the level of the ilium. (1) Ilium; (2) sacrum; (3) gluteus minimus; (4) gluteus medius; (5) gluteus maximus; (6) iliopsoas (iliacus); (7) rectus abdominis; (8) piriformis; (9) external iliac artery; (10) external iliac vein; (11) internal iliac artery; (12) internal iliac vein; (13) superior gluteal artery; (14) inferior epigastric artery; (15) gluteal nerve; (16) femoral nerve; *P posterior*

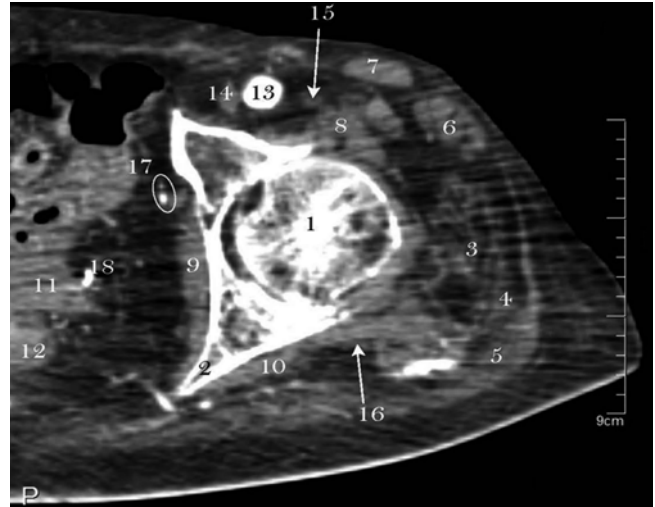


Fig. 32.29 Axial MDCT reconstruction of the arterial phase of MPMCTA at the level of the hip joint. (1) Femur head; (2) sciatic spine; (3) gluteus minimus; (4) gluteus medius; (5) gluteus maximus; (6) tensor fasciae latae; (7) sartorius; (8) iliopsoas; (9) obturator internus; (10) gemelli superior; (11) uterus; (12) rectum; (13) femoral artery; (14) femoral vein; (15) femoral nerve; (16) sciatic nerve; (17) obturator artery; (18) uterine artery; *P posterior*



Fig. 32.28 Horizontal slice of the same pelvis at the level of the ilium. (1) Ilium; (2) sacrum; (3) gluteus minimus; (4) gluteus medius; (5) gluteus maximus; (6) iliopsoas (iliacus); (7) rectus abdominis; (8) piriformis; (9) external iliac artery; (10) external iliac vein; (11) internal iliac artery; (12) internal iliac vein; (13) superior gluteal artery; (14) inferior epigastric artery and vein; (15) gluteal nerve; (16) femoral nerve

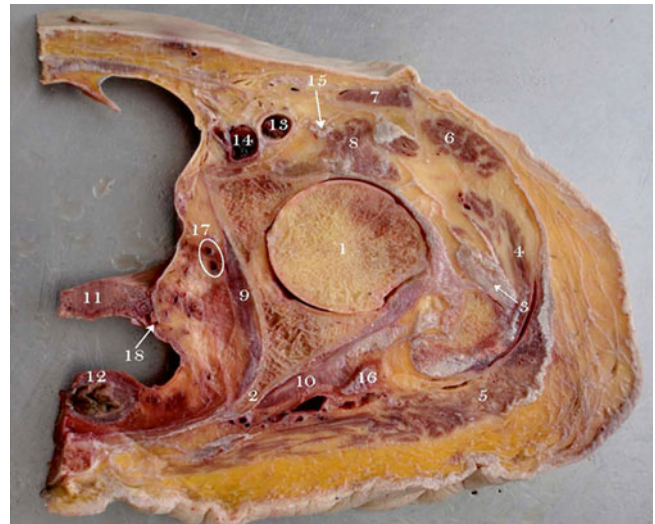


Fig. 32.30 Horizontal slices of the same pelvis at the level of the hip joint. (1) Femur head; (2) sciatic spine; (3) gluteus maximus; (4) gluteus medius; (5) gluteus maximus; (6) tensor fasciae latae; (7) sartorius; (8) iliopsoas; (9) obturator internus; (10) gemelli superior; (11) uterus; (12) rectum; (13) femoral artery; (14) femoral vein; (15) femoral nerve; (16) sciatic nerve; (17) obturator artery; (18) uterine artery



Fig. 32.31 Axial MDCT reconstruction of the arterial phase of MPMCTA at the level of the trochanter minor. (1) Femur (trochanter minor); (2) gluteal maximus; (3) vastus lateralis (quadriceps femoris); (4) vastus intermedius; (5) tensor fasciae latae; (6) rectus femoris; (7) sartorius; (8) iliopsoas; (9) pectineus; (10) adductor longus; (11) adductor brevis; (12) adductor magnus; (13) ischiocavernosus; (14) biceps femoris and semitendinosus; (15) urethra; (16) vagina; (17) anus (sphincter); (18) femoral artery; (19) femoral vein; (20) deep femoral artery; (21) deep femoral vein; (22) greater saphenous vein; (23) femoral nerves; (24) sciatic nerve; (25) pudendal artery, vein, and nerve; * location of ischioanal fossa

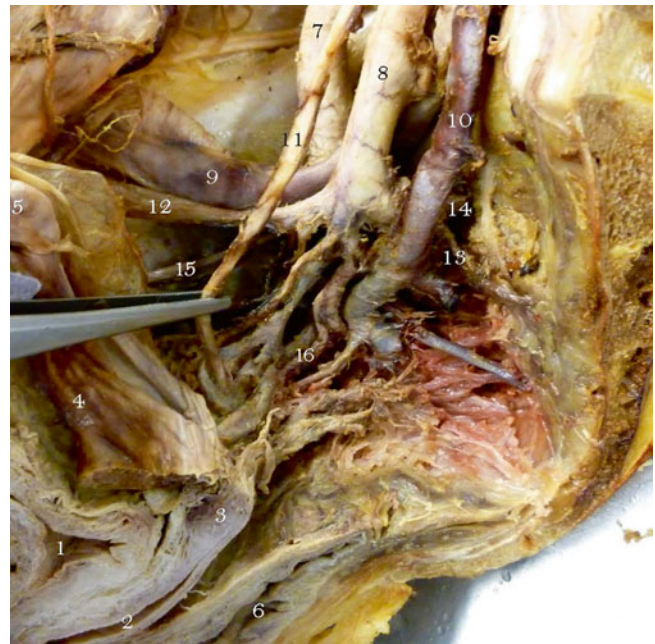


Fig. 32.33 Dissected right hemipelvis. (1) Bladder; (2) vagina; (3) uterus; (4) uterine tube; (5) ovary; (6) rectum; (7) external iliac artery; (8) internal iliac artery; (9) external iliac vein; (10) internal iliac vein; (11) ureter; (12) medial umbilical ligament; (13) lateral sacral artery; (14) superior gluteal artery; (15) obturator artery; (16) uterine artery



Fig. 32.32 Horizontal slices of the same pelvis at the level of the trochanter minor. (1) Femur (trochanter minor); (2) gluteal maximus; (3) vastus lateralis (quadriceps femoris); (4) vastus intermedius; (5) tensor fasciae latae; (6) rectus femoris; (7) sartorius; (8) iliopsoas; (9) pectineus; (10) adductor longus; (11) adductor brevis; (12) adductor magnus; (13) ischiocavernosus; (14) biceps femoris and semitendinosus; (15) urethra; (16) vagina; (17) anus (sphincter); (18) femoral artery; (19) femoral vein; (20) deep femoral artery; (21) deep femoral vein; (22) greater saphenous vein; (23) femoral nerves; (24) sciatic nerve; (25) pudendal artery, vein, and nerve; * location of ischioanal fossa

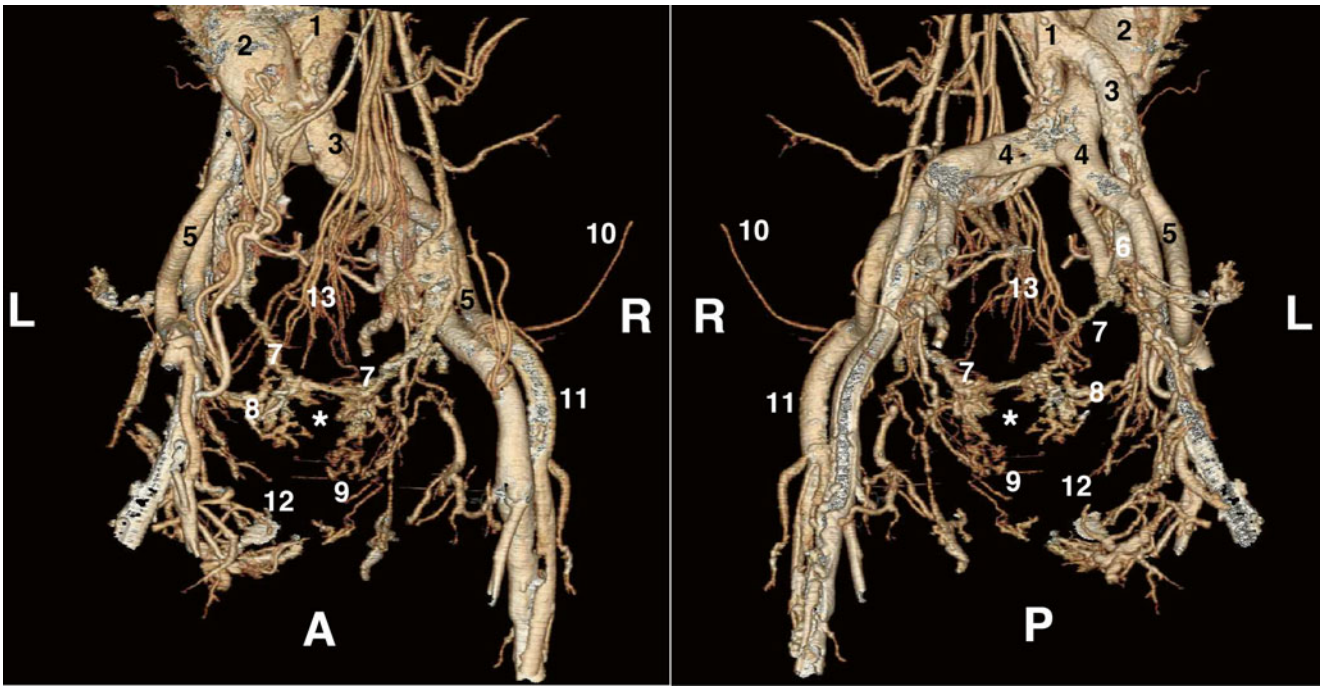


Fig. 32.34 3D-VR reconstruction of blood vessels of the pelvis obtained from the dynamic phase of MPMCTA showing the arteries and veins in an anterior view (*left*) and a posterior view (*right*). (1) Abdominal aorta; (2) vena cava; (3) iliac artery; (4) iliac vein; (5) external iliac artery; (6)

internal iliac artery; (7) inferior rectal artery and veins; (8) accessory inferior rectal artery and veins; (9) perineal and posterior labial blood vessels; (10) superficial iliac artery; (11) femoral artery; (12) anterior labial blood vessels, (13) intestinal arteries; * *location of anus*

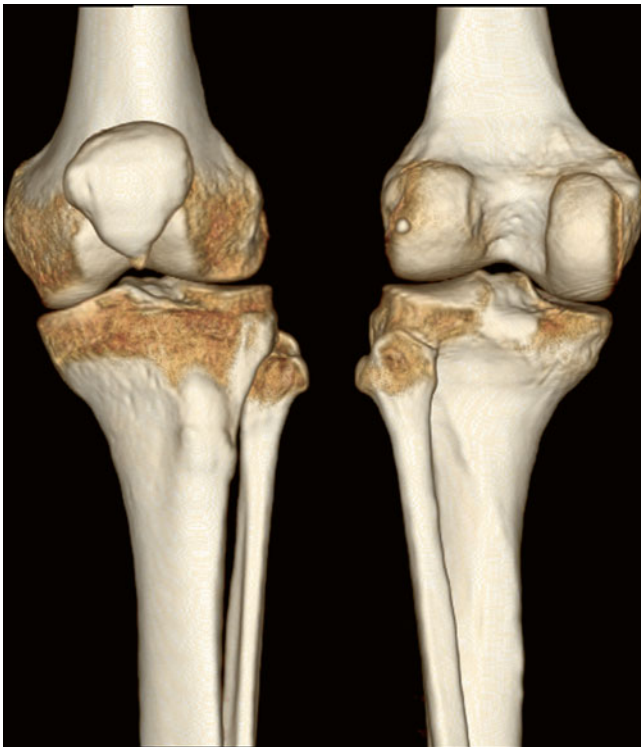


Fig. 32.35 3D-VR reconstruction of bony structures of the knee obtained from a native MDCT. Femur, patella, tibia, and fibula; *anterior view to the left and posterior view to the right*

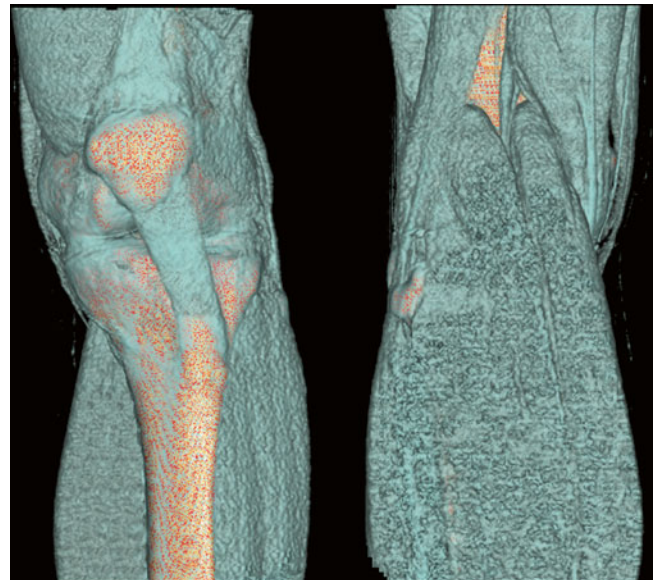


Fig. 32.36 The same knee seen with soft tissue 3D-VR reconstruction showing muscles and ligaments

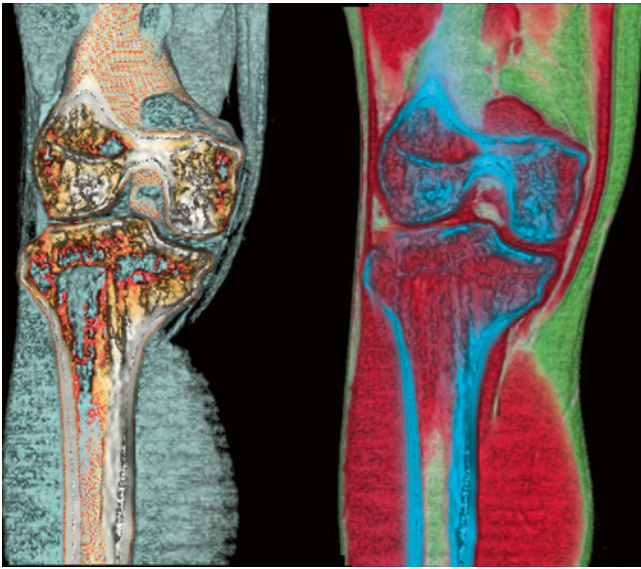


Fig. 32.37 The same knee in frontal cross-sections of a soft tissue 3D-VR reconstruction using different color algorithms

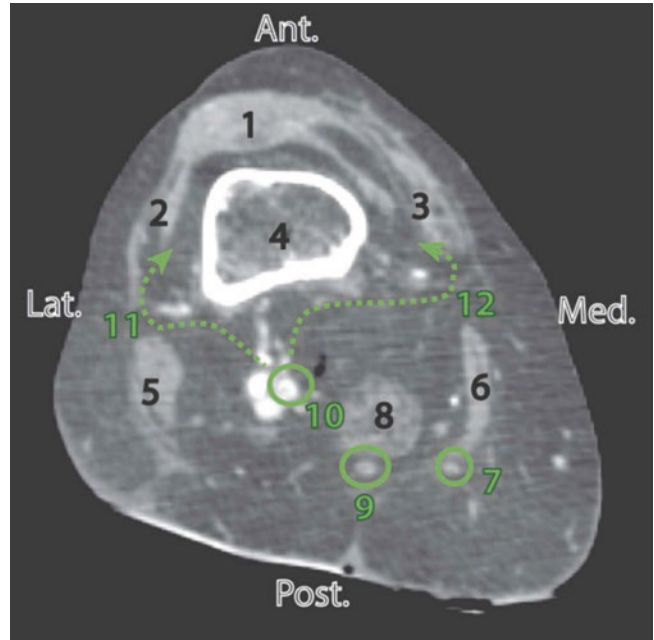


Fig. 32.39 Axial reconstruction of venous phase of MPMCTA of the knee. (1) Patella; (2) vastus lateralis; (3) vastus medialis; (4) femur; (5) biceps femoralis; (6) sartorius; (7) gracilis; (8) semimembranosus; (9) semitendinosus; (10) popliteal artery; (11) lateral superior genicular artery; (12) medial superior genicular artery (the trajectory of both arteries is indicated by arrows)

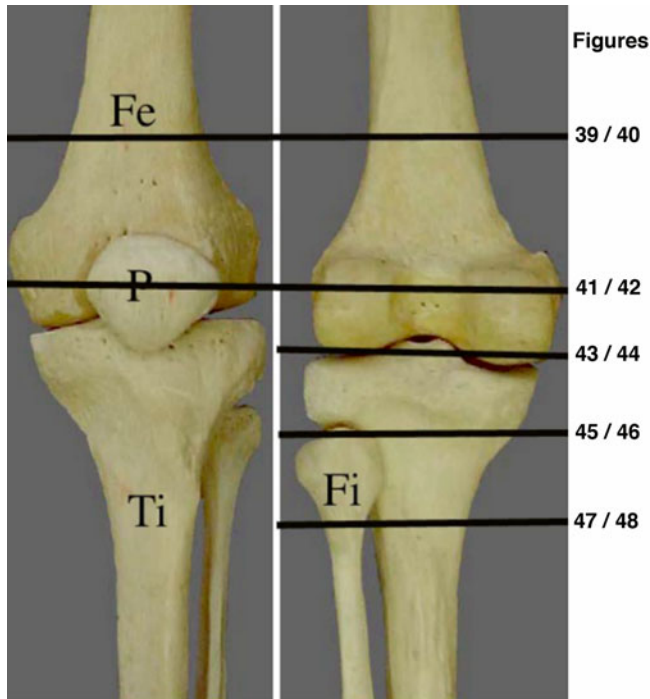


Fig. 32.38 Bony structures of the knee. Femur, patella, tibia, and fibula, anterior view to the left and posterior view to the right. Levels of horizontal CT scans and corresponding slices are indicated and correspond to Figs. 32.39, 32.40, 32.41, 32.42, 32.43, 32.44, 32.45, 32.46, 32.47, and 32.48

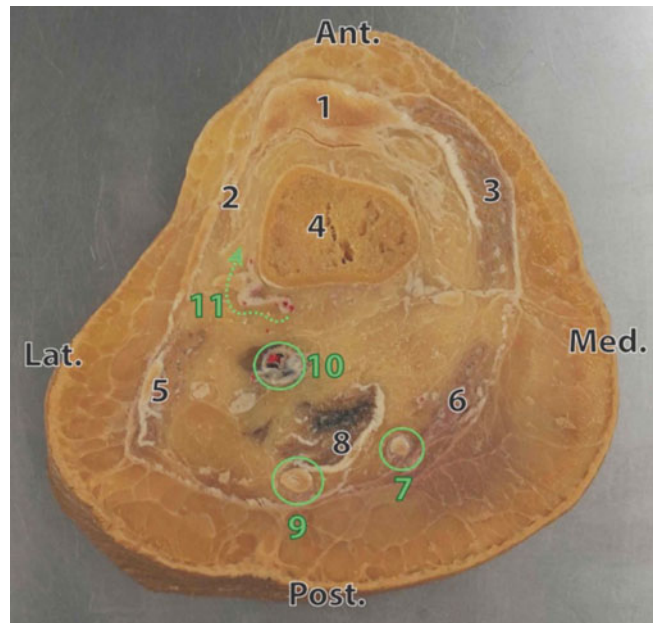


Fig. 32.40 Corresponding horizontal slice of the knee. (1) Patella; (2) vastus lateralis; (3) vastus medialis; (4) femur; (5) biceps femoralis; (6) sartorius; (7) gracilis; (8) semimembranosus; (9) semitendinosus; (10) popliteal vein and artery; (11) descending genicular artery (its trajectory is indicated by an arrow)

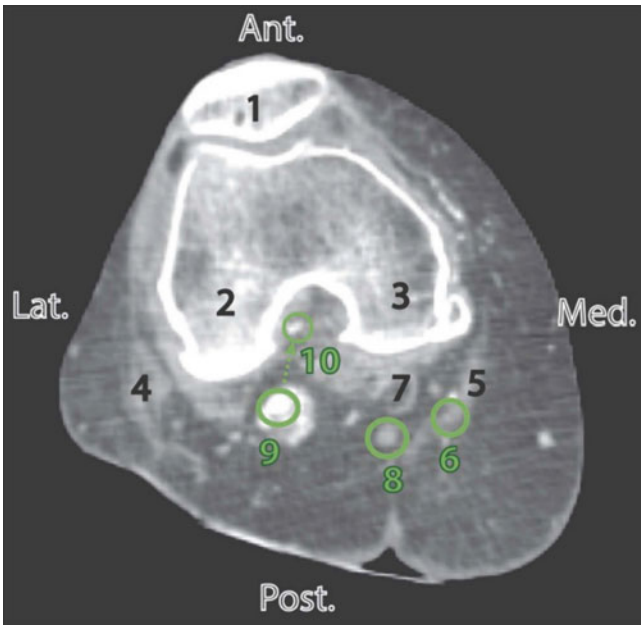


Fig. 32.41 Axial reconstruction of venous phase of MPMCTA of the knee. (1) Patella; (2) lateral condylus; (3) medial condylus; (4) biceps femoralis; (5) sartorius; (6) gracilis; (7) semimembranosus; (8) semitendinosus; (9) popliteal artery; (10) medial genicular artery (arrow)

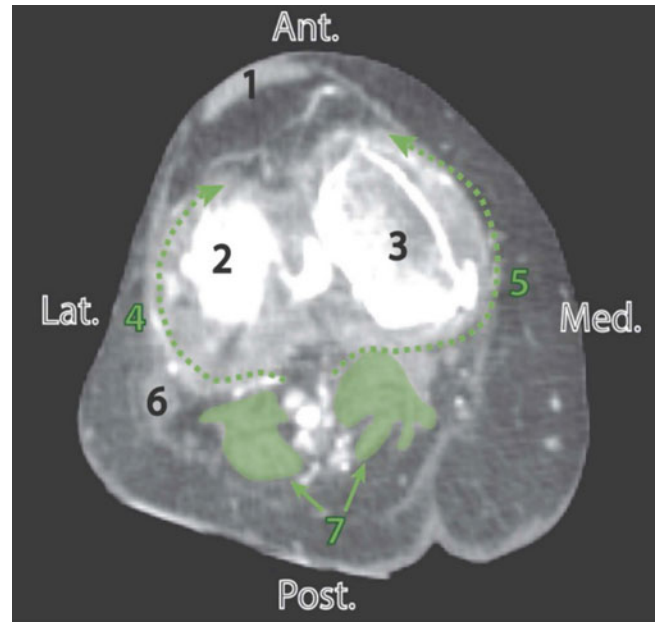


Fig. 32.43 Axial reconstruction of venous phase of MPMCTA of the knee. (1) Patellar ligament; (2) lateral condylus; (3) medial condylus; (4) lateral superior genicular artery; (5) medial superior genicular artery; (6) biceps femoris (tendon); (7) gastrocnemius

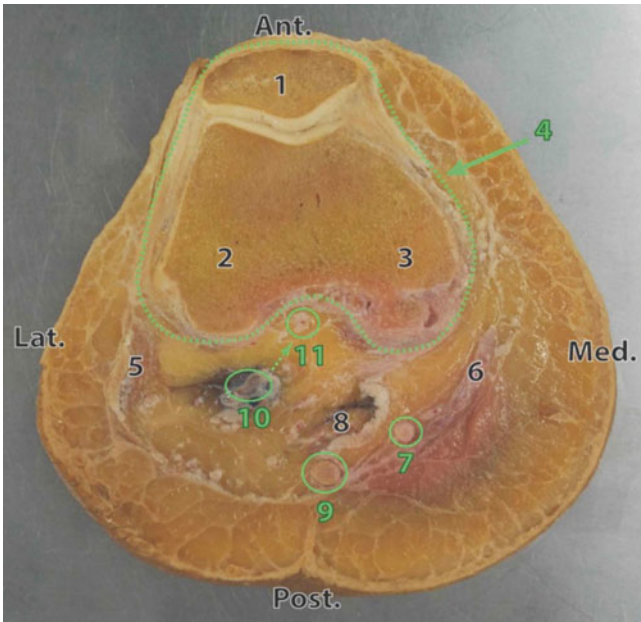


Fig. 32.42 Corresponding horizontal slice of the knee. (1) Patella; (2) lateral condylus; (3) medial condylus; (4) joint capsule (indicated by *pointed line*); (5) biceps femoralis; (6) sartorius; (7) gracilis; (8) semitendinosus; (9) semimembranosus; (10) popliteal artery; (11) medial genicular artery

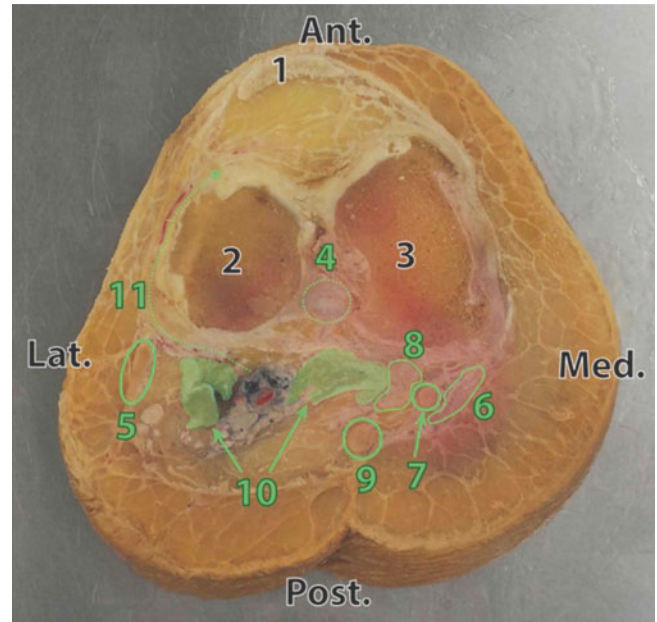


Fig. 32.44 Corresponding horizontal slice of the knee. (1) Patellar ligament; (2) lateral condylus; (3) medial condylus; (4) cruciate ligament; (5) biceps femoris; (6) sartorius; (7) gracilis; (8) semimembranosus; (9) semitendinosus; (10) lateral and medial gastrocnemius; (11) lateral superior genicular artery (both arteries are indicated by *pointed arrows*). Note that the lateral superior genicular artery was filled with red two-component lacquer

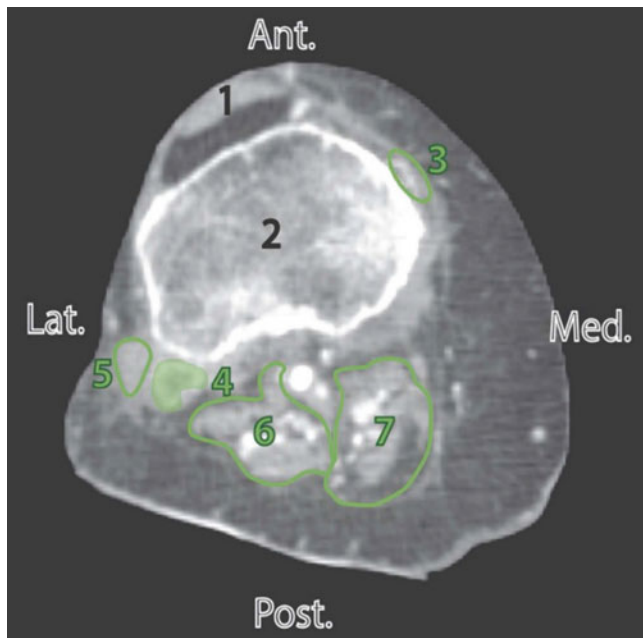


Fig. 32.45 Axial reconstruction of venous phase of MPMCTA of the knee. (1) Patellar ligament; (2) tibial plateau; (3) tibial collateral ligament; (4) fibular head; (5) fibular collateral ligament; (6) lateral gastrocnemius; (7) medial gastrocnemius

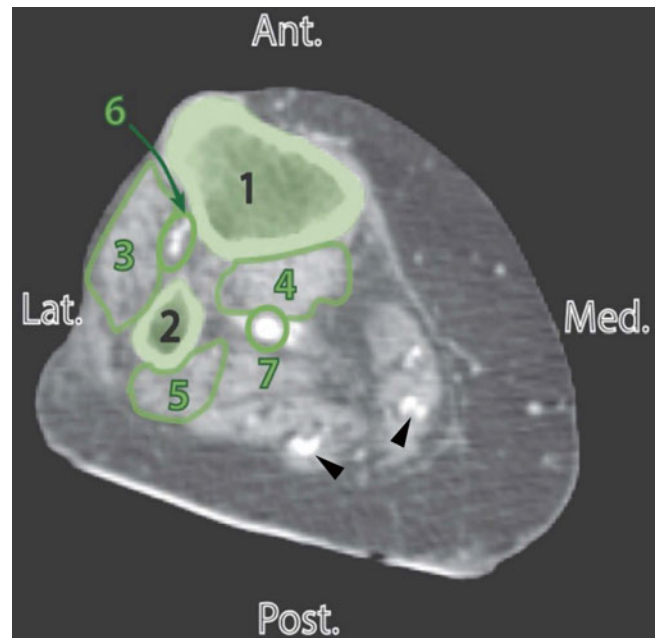


Fig. 32.47 Axial reconstruction of venous phase of MPMCTA of the knee. (1) Tibia; (2) fibula; (3) tibialis anterior; (4) flexor longus digitorum; (5) soleus; (6) anterior tibial artery; (7) posterior tibial artery. Note the muscular blood vessels in the gastrocnemius muscles (arrows)

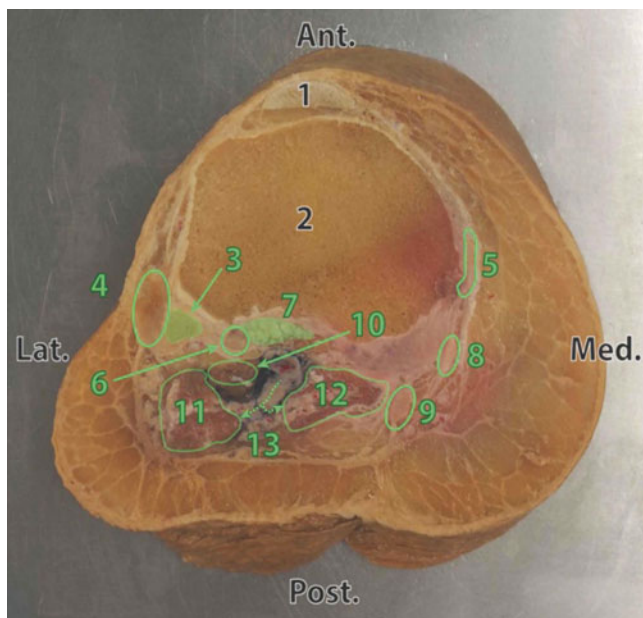


Fig. 32.46 Corresponding horizontal slice of the knee. (1) Patellar ligament; (2) tibial plateau; (3) fibular head; (4) tibial collateral ligament; (5) fibular collateral ligament; (6) popliteus tendon; (7) posterior cruciate ligament; (8) sartorius; (9) semitendinosus; (10) plantaris; (11) lateral gastrocnemius; (12) medial gastrocnemius; (13) including sural arteries (arrowheads)

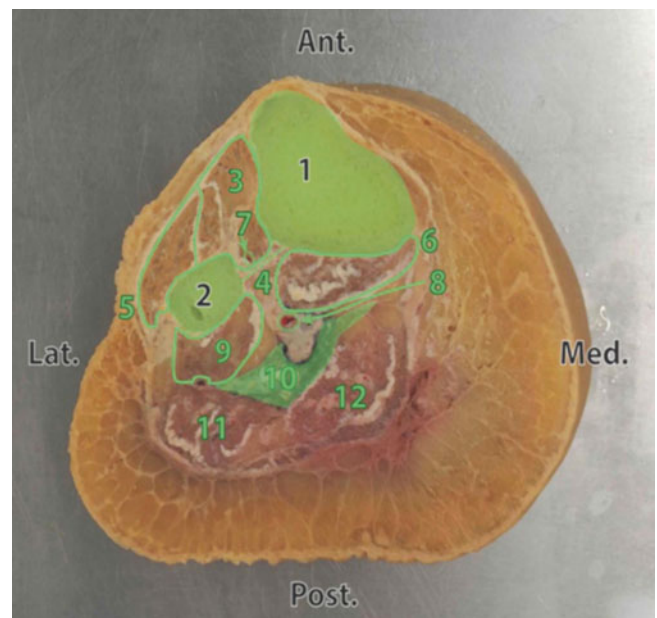


Fig. 32.48 Corresponding horizontal slice of the knee. (1) Tibia; (2) fibula; (3) tibialis anterior and extensor longus digitorum; (4) tibialis posterior; (5) fibularis longus; (6) flexor longus digitorum; (7) anterior tibial artery; (8) posterior tibial artery; (9) flexor longus hallucis; (10) soleus; (11) lateral gastrocnemius; (12) medial gastrocnemius; interosseus membrane (dotted line). Note the muscular blood vessels in the gastrocnemius muscles (red spots)



Fig. 32.49 Sagittal MIP reconstruction of the arterial phase of MPMCTA of the knee. (1) Popliteal artery; (2) lateral superior genicular artery; (3) lateral inferior genicular artery; (4) anterior tibial artery; (5) fibular artery; (6) posterior tibial artery

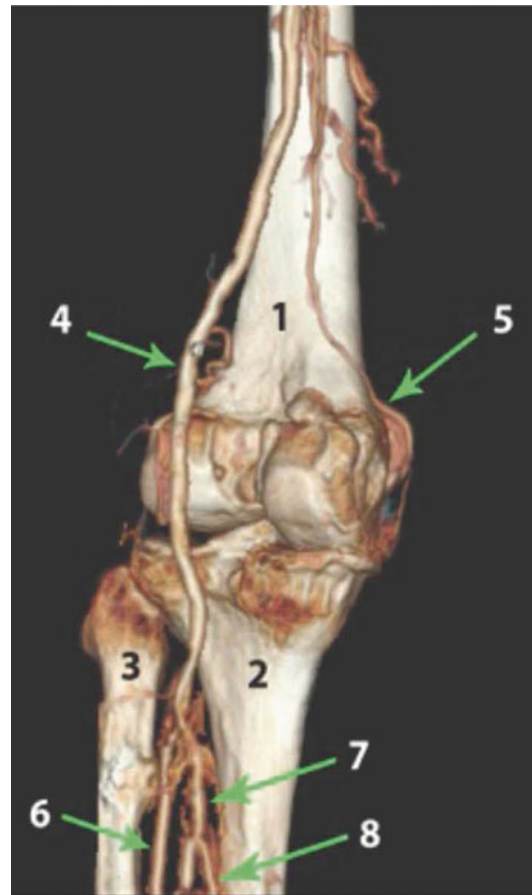


Fig. 32.50 3D-VR reconstruction of the arterial phase of MPMCTA of the knee. (1) Femur; (2) tibia; (3) fibula; (4) popliteal artery; (5) descending genicular artery; (6) anterior tibial artery; (7) posterior tibial artery; (8) fibular artery. Note that the reconstruction of the superior middle and inferior genicular arteries is difficult

32.4 Discussion and Conclusions

In anatomy, the main objective is to identify major anatomic structures, their normal morphology by a detailed view, and even some particulars. An exposure to radiographic images is essential in undergraduate teaching because CT and MRI images can be compared to the real slices with their color and texture, facilitating the identification of the anatomic counterparts in digital CT and MRI scans with their gray levels. It is evident that nervous structures are not detectable on MRI and CT scans, but their location may be inferred by the location of blood vessels. Two organs, the brain and heart, are of special importance in angiography; thus, it is important to get acquainted early in medical learning with angiograms of the brain blood vessels and coronary arteries.

Our previous work has focused on the pelvic floor, the importance of the anatomy for the understanding of deficits such as stress-induced urinary incontinence [31], and how to improve teaching of the pelvic floor to undergraduate students [8]. The recent development of postmortem angiography at Lausanne created an opportunity to apply this technique for clinically related anatomy. For two Master's theses in medicine [1, 2], we used two female bodies to set up CT scans for both bodies, with subsequent reconstruction of bony structures or blood vessels and MRI for comparison. These students had little previous exposure to this kind of imaging, and preparing sets of images for undergraduate teaching was a very good experience (Figs. 32.51 and 32.52). When they presented their work to students in self-directed learning, it rapidly became clear that for comparing two sets of images, students need some guidance (orientation and 3D thinking). Some students felt that they were not sufficiently prepared for an interpretation of radiologic sections, confirming the need to introduce this subject in the first year. Therefore, in a follow-up project, the vascularization of the knee was prepared [3], and most recently of the brachial plexus [4]. When presenting imaging to undergraduate students, it is essential to highlight their clinical importance to emphasize why it is relevant to learn human anatomy. The vascularization of the knee is important, and physicians are confronted with arteriopathies of the lower limb that may obstruct these arteries, such as atherosclerosis. The popliteal artery is concerned in 2.5 % of the population in the age range of 50–59 years, 4.7 % of those 60–69 years old, and more than 14.5 % of those over age 70 years [32], with risk factors such as smoking, obesity, diabetes, hypertension, or high cholesterol levels [33–36]. Placement of balloons and stents to open up stenosis and keep arteries open is quite common [37]. However, the placement of a stent may be problematic in the knee region because of the movements of flexion and extension, with an increased risk of stent rupture [38, 39]. Reports on variations in the vascularization of the knee are scarce. One study indicates that the medial condyle

of the tibia is poorer in its vascularization [40], which may explain the occurrence of ischemic growth disorders following fulminating purpura [41].

At the University of Lausanne, the locomotor system is taught in the first year to medical students, including innervation, muscle function, biomechanics, synapse physiology, and an introduction to the nervous system. Sections and preparations were introduced into self-directed learning sessions and were appreciated by the students. Nevertheless, there was also a need to guide the students in the analysis of radiologic data by assistants and faculty. Parts of the images were also introduced into a newly created e-learning program as a complementary opportunity to consult labeled and unlabeled anatomic specimens after the sessions. The advantage is that this web-based system can be consulted at any time and is not linked to teaching hours of self-directed and dissection sessions. Teaching of anatomy at Lausanne, as is the case in many other Swiss universities, has seen a tremendous change. Along with traditional dissection, in which dissection hours had to be shortened considerably, other teaching tools had to be developed, such as self-directed learning with the use of prosected and plastinated specimens and an elaboration of specific topics of complicated regions such as the pelvis or the neck region. Postmortem angiography adds another modality to multimodal anatomy teaching. Multimodal teaching forms have changed anatomy learning from a passive to an active experience [7]. The use of 3D angiography in combination with scans and anatomic slices of the same cadaver adds an additional form of learning of complex structures such as the vascular system. It also documents the variability of the human body with regard to vascularization. In clinics, the use of angiograms is quite common; therefore, it is essential to introduce students to and prepare them for this type of imaging early in their studies. All four Master's students who prepared these theses and teaching modules confirmed that by preparing the anatomic specimens and comparing scans and slices, they strengthened their learning and retention abilities (Figs. 32.53 and 32.54). Therefore, the introduction of multimodal teaching, especially imaging techniques with their clinical importance, makes it more a necessity than an option that students become familiar with radiographic images and their interpretation. The importance of radiographic imaging in preclinical anatomy teaching has been underlined in a recent publication [42]. It is essential that students match virtual and real anatomic structures. Here I add a comment regarding the multitude of teaching tools. The modular system at Lausanne allows for teaching of the locomotor system in 5 weeks, usually 4 h of lectures and self-directed learning sessions in the afternoons. Students learn at a steady pace, but the density and amount of knowledge to assimilate render it difficult to use the e-learning system in the after hours. Students not only

must memorize the many anatomic structures but also understand why anatomy is important and obtain insight into the clinical context [43]. Students show a similar attitude toward body painting, i.e., painting anatomic structures on the skin, which is judged to be playful but not essential for learning anatomic structures. As with any teaching tool placed at the students' disposal, it should be tailored and

suit to the objectives of each module, and students need to be guided in how to take advantage of the many opportunities for improving their performance in learning. Students must understand the importance of clinical anatomy, both as a scientific and a clinical discipline, and how it relates to issues of understanding of the culture of medicine in terms of health and disease [44].



Fig. 32.51 Medical student teaching the brachial plexus in small groups



Fig. 32.53 Medical student preparing slices of pelvis for photography



Fig. 32.52 Medical student teaching the pelvis in small groups



Fig. 32.54 Preparation of a body for scanning by a medical student

References

- Hoffer N. Etudes anatomique du plancher pelvien en relation avec des complications trouvées en chirurgie gynécologique et proposition d'amélioration de l'enseignement d'une région complexe. [Anatomical study of the pelvic floor in relation to complications found in obstetric surgery and improvement in teaching a complex region]. Master's thesis in medicine, Switzerland: University Lausanne; 2010. p. 1–32.
- Hugonnet I. Etude anatomique du plancher pelvien en relation avec les complications trouvées en chirurgie gynécologique. [Anatomical study of the pelvic floor in relation to complications found in obstetric surgery]. Master's thesis in medicine, Switzerland: University Lausanne; 2011. p. 1–41.
- Ayer R. Etude d'un nouvel outil didactique pour l'apprentissage de la vascularisation du genou en première année de médecine. [Study of a novel didactic tool for learning the vascularization of the knee during the first year of medical studies]. Master's thesis, FBM, Switzerland: Université de Lausanne; 2013.
- Huguenin A. Imagerie et dissection du plexus brachial. [Imaging and dissection of the brachial plexus]. Master's thesis, FBM, Switzerland: Université de Lausanne; 2014.
- Sugand K, Abrahams P, Khurana A. The anatomy of anatomy. A review for its modernization. *Anat Sci Educ.* 2010;3:83–93.
- Zumwalt AC, Lufner RS, Monteiro J, Shaffer K. Building the body: active learning laboratories that emphasize practical aspects of anatomy and integration with radiology. *Anat Sci Educ.* 2010;3:134–40.
- Drake R, Pawlina W. Multimodal education in anatomy: the perfect opportunity. *Anat Sci Educ.* 2014;7:1–2.
- Riederer BM, Spinosa J-P. Teaching clinical anatomy of the female pelvic floor to undergraduate students: a critical review of neuralgic points. *Anatomy.* 2011;5:1–5.
- Riederer BM. Plastination and its importance in teaching anatomy. Critical points for long-term preservation of human tissue. *J Anat.* 2014;224:309–15.
- Cornwall J, Stringer MD. Are computed tomography scans of cadavers perceived as a useful educational adjunct in a surgical anatomy course? *Anat Sci Educ.* 2014;7:77.
- Nwachukwu CR. Cadaver CT, scans a useful adjunct in gross anatomy: the medical student perspectives. *Anat Sci Educ.* 2014;7:83–4.
- Rizzolo LJ, Rando WC, O'Brien MK, Haims AH, Abrahams JJ, Stewart WB. Design, implementation, and evaluation of an innovative anatomy course. *Anat Sci Educ.* 2010;3:109–20.
- Pabst R, Rothkötter HJ. Retrospective evaluation of undergraduate medical education by doctors at the end of their residency in hospitals: consequences for the anatomical curriculum. *Anat Rec.* 1997;249:431–4.
- Pabst R. Anatomy curriculum for medical students: what can be learned for future curricula from evaluations and questionnaires completed by students, anatomists and clinicians in different countries. *Ann Anat.* 2009;191:541–6.
- Kato Y, Sano H, Katada K, Oqura Y, Hayakawa M, Kanaoka N, Kanno T. Application of three-dimensional CT angiography (3D-CTA) to cerebral aneurysm. *Surg Neurol.* 1999;52:121–2.
- Matsumoto M, Kodama N, Endo Y, Sakuma J, Suzuki K, Sasaki T, et al. Dynamic 3D-CT angiography. *Am J Neuroradiol.* 2006;28:299–304.
- Solomon SB, Dickfeld T, Calkins H. Real-time cardiac catheter navigation on three-dimensional CT images. *J Interv Card Electrophysiol.* 2003;8:27–36.
- Grabherr S, Djonov V, Yen K, Thali MJ, Dirnhofer R. Postmortem angiography: review of former and current methods. *Am J Radiol.* 2007;188:832–8.
- Grabherr S, Mangin P, Dominguez A. L'angio-CT post-mortem: un nouvel outil diagnostique [Postmortem Angio-CT : a novel diagnostic tool]. *Rev Med Suisse.* 2011;7:1507–10.
- Grabherr S, Grimm J, Dominguez A, Vanhaebost J, Mangin P. Advances in post-mortem CT-angiography. *Br J Radiol.* 2014;87:1036.
- Musumeci E, Duvoisin B, Lang FJW, Riederer BM. Plastinated ethmoidal region: I. Preparation and applications in clinical teaching. *J Int Soc Plast.* 2003;18:23–8.
- Musumeci E, Lang FJW, Duvoisin B, Riederer BM. Plastinated ethmoidal region: II. The preparation and use of radio-opaque artery casts in clinical teaching. *J Int Soc Plast.* 2003;18:29–33.
- vonHagens G. Heidelberg Plastination Folder. Heidelberg: Anatomisches Institut I, Universität Heidelberg; Tho.Grigg; 1985–1986.
- Willis T. *Cerebri Anatome.* London: 1664.
- Sinclair HM, Robb-Smith AHT. A history of the teaching of anatomy in Oxford. Oxford: University Press; 1950.
- Xavier AR, Qureshi AI, Kirmani JF, Yahia AM, Bakshi R. Neuroimaging of stroke: a review. *South Med J.* 2003;96:4–6.
- Beco J, Klimov D, Bex M. Pudendal nerve decompression in perineology: a case series. *BMC Surg.* 2004;4:15.
- Shafik A, Ahmed I, Shafik AA, El-Ghamrawy TA, El-Sibai O. Surgical anatomy of the perineal muscles and their role in perineal disorders. *Anat Sci Int.* 2005;80:167–71.
- Spinosa J-P, Dubuis PY, Riederer BM. Transobturator surgery for female stress incontinence: a comparative anatomical study outside-in vs inside-out techniques. *BJU Int.* 2007;100:1097–110.
- Spinosa J-P, Laurençon J, Kuhn G. Differential staged sacral reflexes allow a localization of pudendal neuralgia. *Pelvi-périnéologie.* 2009;28:24–8.
- Spinosa J-P, Riederer BM. De l'importance de l'anatomie [on the importance of anatomy]. *L'agenda Gynecologie.* 2007;49:6–8.
- Smith SCJ, Benjamin EJ, Bonow RO, Braun LT, Creager MA, Franklin BA. World Heart Federation and the preventive cardiovascular nurses association. AHA/ACCF secondary prevention and risk reduction therapy for patients with coronary and other atherosclerotic vascular diseases: 2011 update: a guideline from the American Heart Association and American College of Cardiology Foundation. *Circulation.* 2011;124:2458–73.
- Pekkanen J, Linn S, Heiss G, Suchindran CM, Leon A, Rifkind BM, Tyroler HA. Ten-year mortality from cardiovascular disease in relation to cholesterol level among men with and without preexisting cardiovascular disease. *N Engl J Med.* 1990;322:1700–7.
- Vasan RS, Larson MG, Leip EP, Evans JC, O'Donnell CJ, Kannel WB, Levy D. Impact of high normal blood pressure on the risk of cardiovascular disease. *N Engl J Med.* 2001;345:1291–7.
- Critchley JA, Capewell S. Mortality risk reduction associated with smoking cessation in patients with coronary heart disease: a systematic review. *JAMA.* 2003;290:86–97.
- Krauss RM, Winston M, Fletcher RN, Grundy SM. Obesity: impact of cardiovascular disease. *Circulation.* 1998;98:1472–6.
- Becker GJ, Katzen BT, Dake MD. Noncoronary angioplasty. *Radiology.* 1989;170(3 Pt 2):92140.
- Tamashiro GA, Tamashiro A, Villegas MO, Dini AE, Mollón AP, Zelaya DA, et al. Flexion of the popliteal artery: technical considerations of femoropopliteal stenting. *J Invasive Cardiol.* 2011;23:431–3.
- Gardiner GAJ, Stokes KR, Clouse ME, Harrington DP, Bettmann MA. Complications of transluminal angioplasty. *Radiology.* 1986;159:201–8.
- Damsin JP, Zambelli JY, Ma R, Roume J, Colonna F, Hannoun L. Study of the arterial vascularization of the medial tibial condyle in the fetus. *Surg Radiol Anat.* 1995;17:13–7.
- Van der Horst RL. Purpura fulminans—a brief report of three cases. *S Afr Med J.* 1968;XLII:1293–5.
- Riederer BM, Bueno-López JL, Ayer R, Rebelt C, Cadas H, Puyal JP. Practical teaching of preclinical anatomy. *Eur J Anat.* 2015;19:205–13.
- Wilhelmsson N, Dahlgren LO, Hult H, Scheja M, Lonka K, Josephson A. The anatomy of learning anatomy. *Adv Health Sci Educ.* 2010;15:153–65.
- Moxham BJ, Shaw H, Crowson R, Plaisant O. The future of clinical anatomy. *Eur J Anat.* 2011;15:29–46.